Chromatographia (2011) 74:319–325
DOI 10.1007/s10337-011-2069-4

FULL SHORT COMMUNICATION

Experimental and Theoretical Studies on the Enantioseparation and Chiral Recognition of Mandelate and Cyclohexylmandelate on Permethylated β-Cyclodextrin Chiral Stationary Phase

Jie-hua Shi · Zuo-jing Ding · Ying Hu

Received: 21 January 2011 / Revised: 5 May 2011 / Accepted: 9 May 2011 / Published online: 25 May 2011

Abstract Enantioseparations of methyl mandelate (MMA) and methyl α-cyclohexylmandelate (MCHMA) on permethylated β-cyclodextrin (PM-β-CD) chiral stationary phase were explored in detail using high-performance liquid chromatography. The influence of the concentration of organic modifiers, along with the column temperature, was studied. In addition, the thermodynamics parameters of the enantioseparations were determined to discuss driven power in the process of enantioseparations. In addition, host−guest complexation of PM-β-CD with MMA enantiomers was simulated by quantum mechanics PM3 method for understanding the chiral recognition mechanism. The experimental results showed that the retention factor (k), separation factor (α), and resolution factor (Rs) for MMA and MCHMA resolved on the PM-β-CD column all generally decreased with the increase of methanol content, which indicated that the main chiral recognition mechanism is that the hydrophobic portions of MMA and MCHMA are included in the hydrophobic cavity of PM-β-CD to form inclusion complexes. In addition, there is an excellent linear relationship between the logarithms of retention factors (k) of MMA and MCHMA enantiomers and $1/T$. It was demonstrated that the enantioseparations of MMA and MCHMA on PM-β-CD chiral column were enthalpy-driven processes. The modeling results can correctly predict the retention order and provide an atomistic account of how chiral discrimination takes place. It is found that the most stable structure of (*R*)-MMA/PM-β-CD complex is different with that of (*S*)-MMA/PM-β-CD complex. The main driving forces responsible for chiral recognition are hydrophobic forces and weak hydrogen bondings.

Keywords Column liquid chromatography · Mandelate · Cyclohexylmandelate · Permethylated cyclodextrin · Chiral recognition · PM3

J. Shi (✉) · Z. Ding · Y. Hu
College of Pharmaceutical Sciences, Zhejiang University of Technology, Hangzhou 310032, China
e-mail: shijh@zjut.edu.cn

J. Shi
State Key Laboratory Breeding Base of Green Chemistry Synthesis Technology, Zhejiang University of Technology, Hangzhou 310032, China

Introduction

Mandelate and its analogs are important pharmaceutical intermediates, which can be used as raw materials for producing angiotenic including cyclandelate, hydrobenzole and pemoline, bactericide, antispasmodic and so on [1]. As chiral molecules, their optical isomers have different pharmacodynamic action. For example, (*S*)-mandelate is the raw material for producing (*S*)-oxybutynin which is used in the clinical treatment of urgency, urinary frequency and urinary incontinence, and has better pharmacological actions compared with racemic oxybutynin [2, 3]. Thus, the separation of the mandelate enantiomers is necessary to meet the increasing demand for evaluation of the pharmacokinetic attributes of each enantiomer and to control the enantiomeric purity of pharmaceutical preparations. Actually, the researches about enantioseparations of mandelate on cyclodextrin-based CSPs have been reported [3–5]. However, the responsible forces for the most separations are still unknown in detail, so it is of particular interest to get an insight into the mechanism of the separation process.

Cyclodextrins (CDs) are cyclic oligosaccharides consisting of glucose subunits connected through glycosidic

α-1, 4 bond, forming a structure as a hollow truncate with one ring wider than the other [6]. The most common CDs are α-, β- and γ-CD, composing of six, seven and eight glucose units, respectively. Many papers have been published concerning the ability of CDs to form host–guest complexes by including large classes of compounds into their hydrophobic cavities via noncovalent interactions [7–9]. One especially important application of CD-based materials is to separate the enantiomers, which is a natural extension of their inclusion properties. This chiral discrimination ability is mainly caused by the difference in the stability constant of each enantiomer upon complexation with the CDs. In the last decades, although there appeared many separation techniques such as high-performance liquid chromatography (HPLC), gas chromatography (GC), capillary electrophoresis (CE), supercritical fluid chromatography (SFC), capillary electrochromatography (CEC), and micellar electrokinetic capillary chromatography (MEKC), which were used to separate enantiomers by CD-based materials, the mechanisms underlying the separations have not yet been fully clarified due to the limitations of the experimental methods. In these years, molecular modeling represents a very promising tool, which is likely to help us in understanding the chiral recognition processes at atomic levels [10, 11]. In particular, quantum chemical computations are considered as an established method for the prediction of novel structures and properties, which are now being used widely to support experimental work [12]. Computations, using semi-empirical methods like AM1 and PM3, are currently fast enough to make studies of supramolecular and inclusion systems feasible [13–15].

In this work, the enantioseparation of methyl mandelate (MAA) and methyl α-cyclohexylmandelate (MCHMA) on PM-β-CD chiral stationary phase column have been studied by HPLC method. The influence of column temperature and mobile phase on the enantioseparations of MMA and MCHMA has been investigated. The thermodynamic parameters in the process of enantioseparations of MMA and MCHMA on PM-β-CD column were determined to discuss the driven power in the process of enantioseparations. Additionally, the host–guest interaction between PM-β-CD and MMA enantiomers was simulated by semi-empirical PM3 method to discuss the chiral recognition mechanism.

Experimental

Instruments and Reagents

Alliance e2695 series HPLC with 2998 series DAD detector and Empowers workstation were purchased from Waters Corporation (Milford, MA, USA). Nucleosil beta-PM Cyclodextrin column (PM-β-CD) was purchased from Macherey–Nagel Germany). The solvent filter was purchased from Changcheng Glass Instrument factory (Anhui, China). MMA, MCHMA and (*S*)-MCHMA were provided by College of Pharmaceutical Sciences, Zhejiang University of Technology (Zhejiang, China). (*R*)-MMA was purchased from Aladdin Company (Shanghai, China).

HPLC Measurements

The solutes used in this experiment were dissolved by methanol, which were filtered through 0.22 μm filter.

Chromatographic Conditions

The mixture of methanol and water was used as mobile phase; the flow rate was set at 0.5 mL min^{-1}; the sampling volume is 10 μL; the UV detection wavelength is 220 nm. Sodium nitrate was used to determine the t_0 value.

Molecular Modeling

The starting structures of (*R/S*)-MMA enantiomers were constructed with the help of Chem 3D Ultra (Version 8.0, CambridgeSoft com, USA). The initial geometry of PM-β-CD was constructed, using Chem 3D Ultra, from the crystallographic parameters of β-CD taken from the Cambridge structural database (CSD). The H-atoms in all hydroxyl groups of β-CD were replaced with methyl groups. The structures of (*R/S*)-MMA and PM-β-CD were first optimized by MOPAC program implemented in Chem 3D Ultra and then fully optimized using PM3 method implemented in Gaussian 03 until all eigenvalue of the Hessian matrix were positive. The PM3-optimized structures of PM-β-CD and (*R/S*)-MMA were used for the molecular docking calculations.

In order to simulate the inclusion process, the glycosidic oxygens of PM-β-CD were placed onto the *XY* plane and their center was defined as the center of the coordination system. The *Z*-axis was perpendicular to *XY* plane, and the 2-OMe and 3-OMe groups in each glucose unit were placed pointing toward the positive *Z*-axis. The PM-β-CD was then kept in this position while the guest molecules (*R/S*)-MMA were introduced along the *Z*-axis into the PM-β-CD cavity. The (*R/S*)-MMA molecules were docked into the cavity of PM-β-CD as four orientations. The chemical bond linking the chiral carbon to the benzene ring is placed on the *Z*-axis with the carbonyl group pointed toward the positive and negative *Z*-axis, labeled as type 1 and type 2. In addition, the bond linking the chiral carbon and the hydroxyl oxygen is placed on the *Z*-axis with the carbonyl group pointing toward the

negative and positive *Z*-axis, labeled as type 3 and type 4. The relative position between the host and the guest molecule was measured by the distance along the *Z*-axis of the chiral carbon atom (C*) of the guest to the coordination center. Inclusion was emulated by manually moving the guest molecules from 8 to −8 Å, with a stepwise of 1 Å, and a systematic search of the guest molecules around *Z*-axis, from −180° to 180°, was performed using a grid of 30°. These complex geometries were fully optimized by minimizing energy using PM3 method until all eigenvalues of the Hessian matrix were positive. All optimizations were performed in vacuo. The binding energy (BE) upon complexation between MMA and PM-*β*-CD calculated for the minimum energy structures is defined in Eq. (1) [16]:

$$\mathrm{BE} = E(\mathrm{host}-\mathrm{guest})^{\mathrm{opt}} - [E(\mathrm{host})^{\mathrm{opt}} + E(\mathrm{guest})^{\mathrm{opt}}] \quad (1)$$

where, $E(\mathrm{host}-\mathrm{guest})^{\mathrm{opt}}$, $E(\mathrm{host})^{\mathrm{opt}}$, and $E(\mathrm{guest})^{\mathrm{opt}}$ represent the heats of formation of the complex, the free PM-*β*-CD and the free guest, respectively.

Finally, NBO (natural bond orbital) calculation at B3LYP6-31G(d) level for PM3 optimized geometries was carried out in order to elucidate the intermolecular H-bonds between MMA and PM-*β*-CD molecule via the determination the stabilization energy $E^{(2)}$.

Results and Discussion

Influence of Content of Methanol in Mobile Phase

Methanol, ethanol, and acetonitrile, as frequently used organic modifiers in reversed-phase liquid chromatography, were investigated in this study. As shown in Fig. 1, among three kinds of mobile phases with a near solvent eluting power, the methanol–water mixture mobile phase has best separation result on either MMA or MCHMA enantiomers. The results showed that the retention factors (k), separation factor (α) and resolution factor (Rs) for MMA and MCHMA resolved on the PM-*β*-CD column all decreased with the increase of methanol content. Therefore, the main enantiorecognition process is based on the inclusion of the hydrophobic portions of MMA and MCHMA into the hydrophobic cavity of PM-*β*-CD. Baseline enantioseparation for MMA and MCHMA were easily obtained on the PM-*β*-CD column when the methanol content was reduced to 30 (or less) and 75% (or less), respectively (Fig. 1). Considering k and α of the two chiral compounds, methanol:water (20:80 v/v) and methanol:water (65:35 v/v) are the optimal mobile phases to MMA and MCHMA, respectively.

The *R*-isomers of MMA and MCHMA are both eluted earlier than *S*-isomers, determined by injecting pure (*R*)-MMA and (*S*)-MCHMA, respectively. It suggests that the interaction between PM-*β*-CD and the *S*-isomer of MMA and MCHMA is stronger. Lipkowitz et al. [10] reported that MMA enantiomers on *β*-CD chiral stationary phase were separated using HPLC. Compared to the separation figure on the *β*-CD column, it can be seen that the PM-*β*-CD column has better enantioselectivities and higher resolution. The poor ability of native CDs to achieve enantioseparation of guest compounds was supposed to result from the molecular rigidity of these hosts, whereas the loss of intramolecular hydrogen bondings between methoxyl groups in PM-*β*-CD is assumed to improve its capability for chiral recognition [17].

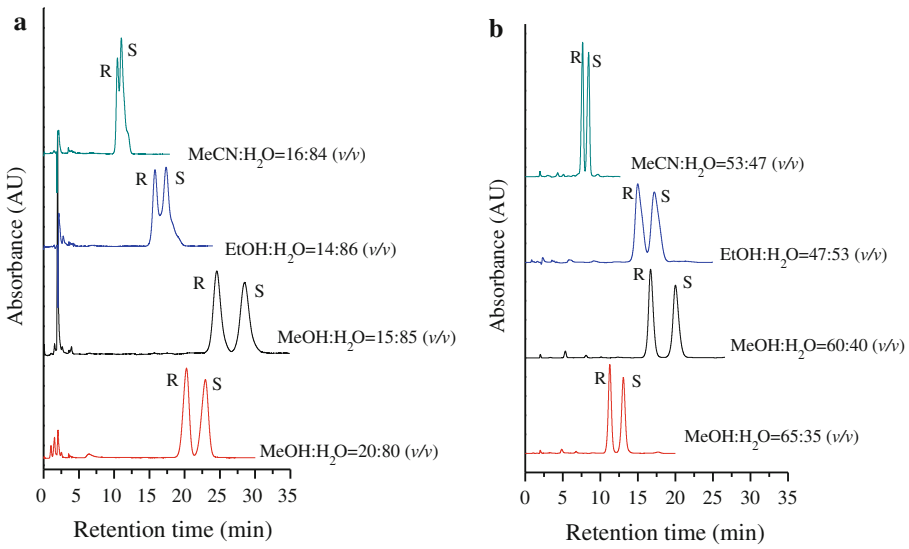

Fig. 1 Chromatograms of the separations of MMA (**a**) and MCHMA (**b**) enantiomers on PM-*β*-CD column, flow rate 0.5 mL min^{-1}; temperature 20 °C

Influence of Column Temperature

The influence of column temperature on their separation was also investigated in the range 15–30 °C with the optimal mobile phases. As expected, the retention time of MMA and MCHMA on PM-β-CD column decreased with the increase of the column temperature, and a concomitant decrease in resolution was found. It can be seen that too high column temperature results in poor separation efficiency, but too low column temperature causes longer retention time. Considering the above phenomenon, the column temperature was set at 20 °C.

Thermodynamic Parameters for Enantiomers Separation

In the process of chromatographic enantioseparation, the relationship between the retention factors (k) or separation factor (α) and the column temperature (T) can be described by the Gibbs–Holmholtz and Van't Hoff equations [18] as follows:

$$\ln k = \frac{-\Delta H}{RT} + \frac{\Delta S}{R} + \ln \varphi \tag{2}$$

$$\ln \alpha = \frac{-\Delta(\Delta G)}{RT} = \frac{-\Delta(\Delta H)}{RT} + \frac{\Delta(\Delta S)}{R} \tag{3}$$

where, k is defined as the retention factors of the solutes. R is gas constant. φ is phase ratio and T is absolute temperature (K). ΔH and ΔS represent, respectively, the enthalpic and entropic contributions of an equilibrium process inside the column. $\Delta(\Delta H)$ and $\Delta(\Delta S)$ represent the differences in the enthalpic and entropic changes for a given pair of enantiomers, respectively. $\Delta(\Delta G)$ represents the free energy of the diastereomeric association equilibria between the chiral selector and the analyte enantiomers. In most cases, the calculated $\Delta(\Delta H)$ value tend to be negative, favoring chiral recognition, the corresponding $\Delta(\Delta S)$ value generally is also negative, counteracting chiral recognition. It indicates that the enantioseparation is enthalpy-driven. Sometimes, for some solutes the $\Delta(\Delta H)$ and $\Delta(\Delta S)$ values are both positive, indicating that the separation is entropy-driven. If the $\Delta(\Delta H)$ value is negative and the $\Delta(\Delta S)$ is positive, the enthalpic and entropic factors are both favorable to chiral recognition [19, 20].

The experimental results showed that the relationship between ln$k$ and 1/T for MAA and MCHMA enantiomers is an excellent linear relationship (Table 1), which indicates that the chiral stationary phase (PM-β-CD) did not change its conformation and enthalpic changes (ΔH) of the MAA and MCHMA enantiomers were invariable over the entire temperature range studied. It was implied that the chiral recognition mechanism for MMA and MCHMA on PM-β-CD column did not change over the entire temperature range studied.

The thermodynamic parameters for MMA and MCHMA enantiomers in chromatographic retention process calculated by Van't Hoff equation are presented in Table 1. It can be seen that the enthalpy changes (ΔH) for MMA and MCHMA in chromatographic retention process on PM-β-CD column were negative, indicating that the interaction between MMA or MCHMA and PM-β-CD stationary phase is exothermic and the transfer of solutes from the mobile phase to the CSP is enthalpically favored. The ($\Delta S + R\ln\varphi$) values of MMA and MCHMA in chromatographic retention process were negative, which is not favorable to the chiral recognition. To ensure the separation of MMA or MCHMA enantiomers [$\Delta(\Delta G) < 0$], therefore, there must be an enthalpic compensation in the process of interaction between MMA or MCHMA and PM-β-CD. Additionally, the difference in the enthalpic and entropic changes of enantiomers of MMA and MCHMA in chromatographic retention process fits with

Table 1 Relationship between ln$k$ and T and thermodynamic parameters for separation of MMA and MCHMA enantiomers

Compounds	$\ln k = \frac{A}{T} + B \quad (r)$[a]			ΔH (kJ mol^{-1})	$\Delta S + R\ln\varphi$ (J mol^{-1} K^{-1})	$\Delta(\Delta H)$[b] (kJ mol^{-1})	$\Delta(\Delta S)$[c] (J mol^{-1} K^{-1})	$\Delta(\Delta G)$[d] (J mol^{-1})
	A	B	r					
MMA								
k_S	2444.9	−6.0994	0.9999	−20.33	−50.71	−2.86	−8.58	−346.06
k_R	2101.6	−5.0671	0.9999	−17.47	−42.13			
MCHMA								
k_S	1987.5	−5.1940	0.9994	−16.53	−43.18	−2.95	−8.52	−453.64
k_R	1633.8	−4.1687	0.9990	−13.58	−34.66			

[a] The equation is relationship between ln$k$ and T, where A equals $\Delta H/R$, B equals $\Delta S/R + \ln\varphi$, r is correlation coefficient. R is gas constant (8.314 J mol^{-1})

[b] $\Delta(\Delta H)$ is determined by the calculation of the difference between ΔH_S and ΔH_R

[c] $\Delta(\Delta S)$ is determined by the calculation of the difference between ($\Delta S_S + R\ln\varphi$) and ($\Delta S_R + R\ln\varphi$)

[d] $\Delta(\Delta G)$ is calculated by $\Delta G = \Delta H - T{\cdot}\Delta S$ at 293 K

$|\Delta(\Delta H)| > |T\Delta(\Delta S)|$ over the entire temperature range studied, which indicates that the enantioseparations of MMA and MCHMA are enthalpy-driven processes.

Molecular Modeling of the Complex of PM-β-CD with Each Enantiomer of MMA

To understand where and how enantiodifferentiation takes place, the interaction between PM-β-CD and each enantiomer of MMA was further investigated using molecular modeling techniques to complement the experimental studies. Considering the large size of the PM-β-CD structure, semi-empirical PM3 method was adopted to further study. As expected, the binding energies of the inclusion complexation of (*R/S*)-MMA into PM-β-CD cavity were changed at different positions (*Z*) and orientations. The more negative the binding energy is, the stronger is the interaction between (*R/S*)-MMA and PM-β-CD, and the more stable is the inclusion complex. The modeling results showed that the binding energies of (*R*)-MMA/PM-β-CD and (*S*)-MMA/PM-β-CD complexes were lowest as (*R/S*)-MMA molecules were included into PM-β-CD at about 4 Å by the orientation of type 3, which are −79.14 and −85.71 kJ mol^{-1}, respectively. It was evidenced that the complexation process is energetically favorable. Also, it can be observed that the BE of (*S*)-MMA/PM-β-CD is more negative than that of (*R*)-MMA/PM-β-CD, which suggests that the interaction of PM-β-CD with (*S*)-MMA is stronger than that with (*R*)-MMA. It is consistent with the elution order observed in the chromatographic experiment, indicating that (*S*)-MMA interacts strongly with PM-β-CD and consequently eluted later. The difference in the interaction energies between the two enantiomers, $\Delta E = 6.57$ kJ mol^{-1}, represents the energetic contribution to enantioselectivity.

The optimized geometries of the inclusion complexes obtained by PM3 calculations are presented in Fig. 2. Although (*R*)-MMA and (*S*)-MMA both lie on the wider edge of the PM-β-CD cavity, the binding geometries of the two complexes are fully different. The benzene ring of (*R*)-MMA locates horizontally approximately on the wider edge of the PM-β-CD cavity with the ester group included into PM-β-CD cavity as the angle between the bond linking the chiral carbon to carbonyl carbon and the *Z*-axis is 54.0°. On the contrary, the ester group of (*S*)-MMA locates horizontally approximately while the benzene ring is deeply included into the hydrophobic cavity as the angle between the bond linking the chiral carbon to the benzene ring and the *Z*-axis is 40.37°. In addition, the carbonyls of (*R/S*)-MMA both point to the up (the wider edge of the PM-β-CD cavity). The shortest distance between the chiral carbon of (*R*)-MMA and the O2 and O3 in the glucose are 4.87 and 5.28 Å, respectively, while the vertical distance between the chiral carbon and the *XY* plane is 3.97 Å. Relatively, the shortest distances between the chiral carbon of (*S*)-MMA and the O2 and O3 in the glucose are 4.80 and 4.05 Å, respectively, while the vertical distance between the chiral carbon and the *XY* plane is 4.17 Å. We can note that, on the most stable structures, the chiral carbon in (*R/S*)-MMA molecule is close to C2, C3 (chiral carbon) in glucose units and the interaction between (*S*)-MMA and PM-β-CD is stronger. It is indicated that the chiral recognition mechanism is closely related to the chiral environment provided by C2 and C3 in the glucose unit and the degree of (*R/S*)-MMA and PM-β-CD inclusion.

Hydrogen Bonding Analysis

In order to have a better estimation of the chiral recognition between (*R/S*)-MMA and PM-β-CD, NBO analysis was carried out to predict H-bond established between host and guest. In NBO analysis, a stabilization energy ($E^{(2)}$) is used to characterize the interaction between the LP(Y) lone pair of the proton acceptor and BD* (X–H) anti-bond of proton donor, which reflects the delocalization trend of electrons from electron donor to acceptor orbitals [21]. It is suggested, in general, that the $E^{(2)}$ value is larger than 8.37 kJ mol^{-1} for strong H-bond interaction and from 8.37 to 2.09 kJ mol^{-1} for weak H-bond interaction [22]. The electron donor orbitals, electron acceptor orbitals and the corresponding $E^{(2)}$ energies, distances and angles of the most stable (*R/S*)-MMA/PM-β-CD complexes optimized by PM3 methods are summarized in the Table 2. The detailed intermolecular H-bonds interactions for the two inclusion complexes are also shown in Fig. 2 as dotted lines. The binding geometries in the two complexes are affected by numerous host–guest C–H···O interactions, resulting from induced fits of the host toward the guests. From Table 2, it can be seen that the stabilization energies ($E^{(2)}$) of C–H···O in both inclusion complexes are less than 8.37 kJ mol^{-1}, indicating that there are two weak H-bonds and three very weak H-bonds in (*R*)-MMA/PM-β-CD inclusion complex, as there are merely three very weak H-bonds in (*S*)-MMA/PM-β-CD inclusion complex. The O···H distances and C–H···O angles of these H-bonds are less than 3.0 Å and greater than 90°, respectively. Interestingly, it is found that the H-bond interaction in (*R*)-MMA/PM-β-CD complex is stronger than that in (*S*)-MMA/PM-β-CD complex. According to the binding energies of the two complexes, however, the host–guest interaction in (*R*)-MMA/PM-β-CD complex is not stronger than that in (*S*)-MMA/PM-β-CD complex. This may be caused by that the aromatic moiety of (*S*)-MMA is included into the hydrophobic cavity of PM-β-CD. According to the above results, it was deduced that the differences of hydrophobic interaction and H-bonds interaction in the inclusion process of (*R/S*)-MMA and PM-β-CD play

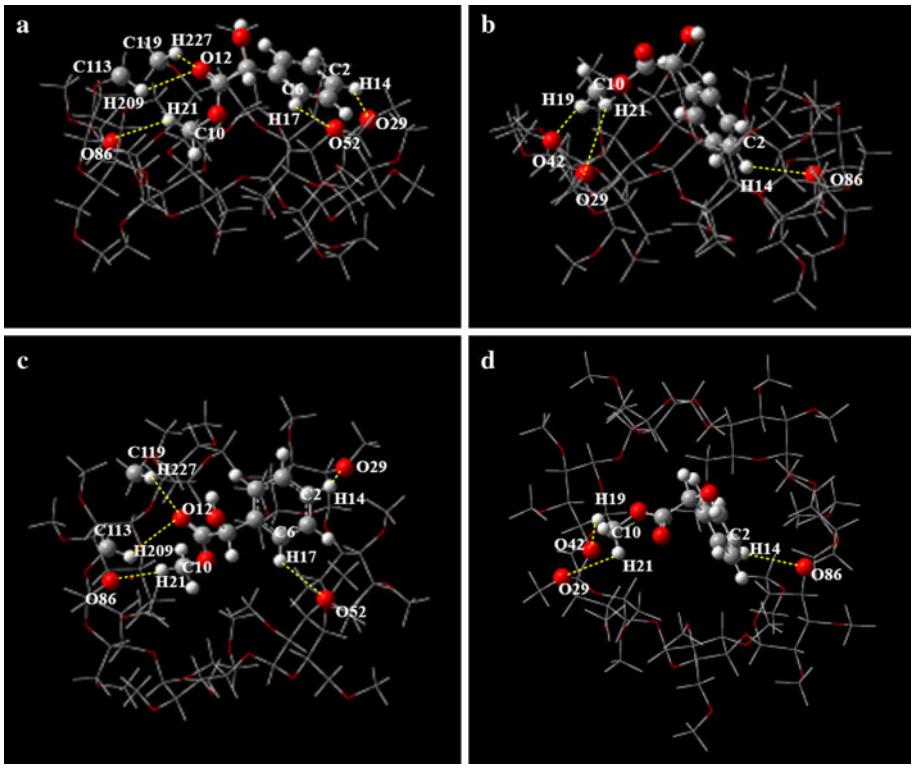

Fig. 2 Energy-minimized structures obtained by PM3 calculations for the (*R/S*)-MMA/PM-*β*-CD complexes. **a** (*R*)-MMA/PM-*β*-CD seen from the side of the PM-*β*-CD wall; **b** (*S*)-MMA/PM-*β*-CD seen from the side of the PM-*β*-CD wall; **c** (*R*)-MMA/PM-*β*-CD seen from the wider edge of the PM-*β*-CD cavity; **d** (*S*)-MMA/PM-*β*-CD seen from the wider edge of the PM-*β*-CD cavity. The possible intermolecular hydrogen bonds with $d_{H\cdots O}$ <3 Å are shown as a dotted line. *O29* and *O52* denote oxygen atoms of 2-OMe and 3-OMe moiety in glucose, respectively. *O42* and *O86* denote glycosidic oxygen atoms. *O12* denotes oxygen atom of carbonyl moiety in MMA

important roles on the chiral recognition of (*R/S*)-MMA and PM-*β*-CD.

Conclusion

A detailed analysis of the host–guest complex between MMA and MCHMA enantiomers with PM-*β*-CD was carried out using chromatography. Particularly, the interaction between PM-*β*-CD and MMA enantiomers was further studied using molecular simulations. In chromatographic studies, the influence of content of methanol in mobile phase and column temperature were investigated, and the optimal separation conditions were given. In addition, thermodynamic parameters at different temperatures were derived by Van't Hoff equation. The more tightly bound enantiomers are both the *S*-isomer. The stereodifferentiating binding energy was found to be enthalpic in nature,

Table 2 The electron donor orbitals, electron acceptor orbitals and the corresponding $E^{(2)}$ energies, distances and angles calculated by NBO analyses at B3LYP/6-31G(d) level for PM3 optimized geometries

Complex	Electron donor[a]	Electron acceptor[b]	*d* (Å)[c]	Angle (°)[d]	$E^{(2)}$ (kJ/mol)[e]
(*R*)-MMA/PM-*β*-CD	LP O12	BD*C119-H227	2.53	143.22	4.64
	LP O12	BD*C113-H209	2.86	120.79	0.38
	LP O29	BD*C2-H14	2.71	132.22	2.34
	LP O52	BD*C6-H17	2.74	130.95	0.63
	LP O86	BD*C10-H21	0.276	120.68	1.21
(*S*)-MMA/PM-*β*-CD	LP O29	BD*C10-H21	2.87	105.03	0.25
	LP O42	BD*C10-H19	2.88	117.57	0.63
	LP O86	BD*C2-H14	2.88	132.23	0.71

The numbers for above atoms are shown in Fig. 2

[a] LP denotes valence lone pair

[b] BD* denotes σ^* antibonding orbital

[c] *d* denotes the O···H distance

[d] Angle means the angel of O···H–C

[e] $E^{(2)}$ means a stabilization energy of interactions between LP and BD* orbitals

almost exclusively. Molecular modeling studies revealed the interaction between MMA and PM-β-CD at the atomic level. The theoretical retention order is in agreement with chromatography, that (*R*)-MMA is eluted first. The results show that it is feasible to predict the elution order of enantiomers by molecular modeling study. The main driven forces responsible for chiral recognition are hydrophobic forces and weak hydrogen bondings.

References

1. Xu GY, Li MH, Liu LL (2000) Pharmaceutical intermediate manual. In: Chemical industry Press, Beijing, pp. 164
2. Xu X, Lan XQ, Yang D, Song H (2007) Chin J Instrum Anal 26:895–897
3. Shi JH, Cheng XW, Yan W (2009) Chin J Pharm Anal 29:1681–1684
4. Ruan YP, Zhang XM, Chen AQ, Qiu HY, Huang PQ (2004) Chin J Chromatogr 22:420–423
5. Nie MY, Zhou LM, Wang QH, Zhu DQ (2000) Chin J Anal Chem 28:1366–1370
6. Szejtli J (1998) Chem Rev 98:1743–1753
7. Yan CL, Xiu ZL, Li XH, Hao C (2007) J Mol Graph Model 26:420–428. doi:10.1016/j.jmgm.2007.01.010
8. Ma SL, Shen S, Haddad N, Tang WJ, Wang J, Lee H, Yee N, Senanayake C, Grinberg N (2009) J Chromatogr A 1216:1232–1240. doi:10.1016/j.chroma.2008.12.016
9. Shi JH, Xiao KK, Lü YY (2009) Acta Phys Chim Sin 25:1273–1278
10. Lipkowitz KB, Stoehr CM (1996) Chirality 8:341–350
11. Shi JH, Yan Y (2010) Chin J Anal Chem 38:1450–1456. doi:10.1016/S1872-2040(09)60072-4
12. Pumera M, Rulíšek L (2006) J Mod Model 12:799–803. doi:10.1007/s00894-005-0082-y
13. Chakraborty S, Basu S, Lahiri A, Basak S (2010) J Mol Struct 977:180–188. doi:10.1016/j.molstruc.2010.05.030
14. Fatiha M, Khatmi DE, Largate L (2010) J Mol Liq 154:1–5. doi:10.1016/j.molliq.2010.03.004
15. Filippa M, Sancho MI, Gasull E (2008) J Pharm Biomed Anal 48:969–973. doi:10.1016/j.jpba.2008.06.005
16. Yahia OA, Khatmi DE (2009) J Mol Struct (Theochem) 912:38–43. doi:10.1016/j.theochem.2009.06.007
17. Grandeury A, Petit S, Gouhier G, Agasse V, Coquerel G (2003) Tetrahedron Asymmetr 14:2143–2152. doi:10.1016/S0957-4166(03)00360-4
18. McGachy NT, Grinberg N, Variankaval N (2005) J Chromatogr A 1064:193–204. doi:10.1016/j.chroma.2004.12.013
19. Lv CG, Zhou ZQ (2011) J Sep Sci 34:363–370. doi:10.1002/jssc.201000762
20. Weng W, Zeng QL, Yao BX, Lin WS, Wang QH, You XL (2006) Chromatographia 64:463–467. doi:10.1365/s10337-006-0040-60009-5893/06/10
21. Madi F, Khatmi D, Dhaoui N, Bouzitouna A, Abdaoui M, Boucekkine A (2009) C R Chimie 12:1305–1312. doi:10.1016/j.crci.2009.06.007
22. Uccello-Barretta G, Balzano F, Sicoli G, Paolino D, Guccione S (2004) Bioorg Med Chem 12:447–458. doi:10.1016/j.bmc.2003.10.033